HHS Public Access

Author manuscript

Isr J Chem. Author manuscript; available in PMC 2025 May 14.

Published in final edited form as:

Isr J Chem. 2024 December ; 64(12): . doi:10.1002/ijch.202300125.

Pharmacologic Targeting of PDIA1 Inhibits NLRP3 Inflammasome Assembly and Activation

Jessica D. Rosarda[a], **Caroline R. Stanton**[a],[b], **Emily B. Chen**[a], **Michael J. Bollong**[b], **R. Luke Wiseman**[a]

[a]Department of Molecular and Cellular Biology, Scripps Research, La Jolla, CA 92037

[b]Department of Chemistry, Scripps Research, La Jolla, CA 92037

Abstract

The NLRP3 inflammasome is a cytosolic protein complex that regulates innate immune signaling in response to diverse pathogenic insults through the proteolytic processing and secretion of pro-inflammatory cytokines such as IL-1β. Hyperactivation of NLRP3 inflammasome signaling is implicated in the onset and pathogenesis of numerous diseases, motivating the discovery of new strategies to suppress NLRP3 inflammasome activity. We sought to define the potential for the proteostasis regulator AA147 to inhibit the assembly and activation of the NLRP3 inflammasome. AA147 is a pro-drug that is metabolically converted to a reactive metabolite at the endoplasmic reticulum (ER) membrane to covalently modify ER-localized proteins such as protein disulfide isomerases (PDIs). We show that AA147 inhibits NLRP3 inflammasome activity in monocytes and monocyte-derived macrophages through a mechanism involving impaired assembly of the active inflammasome complex. This inhibition is mediated through AA147-dependent covalent modification of PDIA1. Genetic depletion or treatment with other highly selective PDIA1 inhibitors similarly blocks NLRP3 inflammasome assembly and activation. Our results identify PDIA1 as a potential therapeutic target to mitigate NLRP3 inflammasome-mediated pro-inflammatory signaling implicated in etiologically diverse diseases.

Keywords

innate immunity; protein disulfide isomerase; inflammasome; NLRP3; small molecule; inhibitor

Introduction

Inflammasomes are multi-protein complexes involved in orchestrating local and systemic innate immune responses to diverse insults.[1–3] While multiple inflammasome complexes

wiseman@scripps.edu .

Author Contributions

JR and CRS conceived, designed, performed, and interpreted the experiments. EC performed and interpreted experiments. MB and RLW conceived and designed experiments and supervised the project. JR wrote the manuscript. CRS, MB, and RLW revised the manuscript and provided approval for submission.

Supporting information for this article is available on the WWW under https://doi.org/10.1002/ijch.202300125

have been identified, activation of the NLR family pyrin domain containing 3 (NLRP3) inflammasome is perhaps the most clearly understood.[3,4] The NLRP3 inflammasome can be activated by a multitude of pathogen- or damage-associated signals which generally involve both a priming and an activating stimulus.[2,3,5] The priming signal induces the NF-κB dependent expression of NLRP3 inflammasome signaling components, while a secondary activation signal then initiates oligomerization of individual components into the functional NLRP3 inflammasome complex (Figure S1A).[3,6,7] Upon assembly and activation, the NLRP3 inflammasome stimulates the maturation and release of pro-inflammatory cytokines such as the highly potent cytokine IL-1β.[1,2,8] Secreted cytokines then promote inflammatory responses that can neutralize threats, although this can also contribute to inflammation-mediated tissue damage.[9,10] Pathologic IL-1β signaling caused by NLRP3 inflammasome hyperactivation has been linked to diverse diseases including cryopyrin-associated periodic syndromes (CAPS),[11,12] type II diabetes mellitus,[9,13,14] as well as cardiac and cerebral ischemia and reperfusion (I/R) injury.[8–10,15,16]

Considering the central importance of the NLRP3 inflammasome in the pathogenesis of disease, therapeutic strategies to inhibit the activation and signaling of this complex has emerged as a highly attractive approach to mitigate inflammation-related pathologies.[7,17–19] In fact, inhibiting the NLRP3 inflammasome and downstream signaling has been shown to reduce tissue damage and improve outcomes in a variety of animal disease models, as well as in human patients.[10,13,16,19,20] Monoclonal antibodies that suppress IL-1β signaling downstream of inflammasome activation are clinically approved to treat several inflammatory diseases and have shown benefits in numerous animal models of inflammatory disorders.[10,13,20,21] Further, numerous pharmacologic strategies have been developed to inhibit NLRP3 inflammasome assembly and activation.[18] Compounds like MCC950 have been shown to bind the ATP binding pocket of NLRP3 to inhibit inflammasome assembly and mitigate pathologic inflammasome signaling in numerous mouse models of inflammatory disease.[15,22–25] Other compounds that bind the NLRP3 ATP binding site, such as OLT1177, have also been tested in clinical trials for inflammatory diseases such as gout and osteoarthritis.[26,27] Despite the promise of these approaches, no direct NLRP3 inflammasome inhibitor is currently approved as a treatment, necessitating the continued development of new pharmacologic strategies to block NLRP3 inflammasome signaling.

Intriguingly, numerous electrophilic compounds have also been found to covalently modify cysteine residues within the NLRP3 inflammasome and inhibit complex assembly. The anti-inflammatory compound oridonin inhibits NLPR3 inflammasome activity through a mechanism predicted to involve selective modification of $NLRP3^{Cys279}$.[28] Similarly, compound RRx-001, which was originally identified as an anticancer compound, is predicted to inhibit inflammasome assembly through covalent modification of $NLRP3^{Cys409}$.[29] Further, itaconate, an immunomodulatory metabolite, is predicted to block inflammasome assembly and activity in mice through modification of $NLRP3^{Cys548}$.[30] More recent screens have identified additional electrophilic compounds that target multiple cysteines residues on NLRP3 to inhibit inflammasome assembly and activity, indicating that NLRP3 is a major electrophilic sensor within the cell.[31]

We previously identified compound AA147 as a highly-selective regulator of endoplasmic reticulum (ER) proteostasis.[32] We showed that the 2-amino-p-cresol moiety of AA147 is metabolically activated at the ER membrane to a reactive electrophile that selectively modifies proteins localized near the ER membrane, such as protein disulfide isomerases (PDIs).[33] AA147-dependent PDI modification can both directly influence ER proteostasis for destabilized proteins such as immunoglobulin light chains[34] and induce adaptive ER proteostasis remodeling through activation of the ATF6 signaling arm of the unfolded protein response.[32] Previous results suggest that the NLRP3 inflammasome assembles at the ER membrane.[35] Considering the electrophilic sensing activity of NLRP3,[31] we predicted that local, metabolic activation of AA147 to a reactive electrophile could potentially inhibit NLRP3 inflammasome assembly and activity through direct targeting of NLRP3 cysteine residues.[31,36] Supporting this prediction, we previously showed that AA147 covalently modifies the electrophilic sensor KEAP1 to activate NRF2 signaling in neuronal cell models through a similar mechanism.[36]

Here, we found that AA147 is a potent and effective inhibitor of NLRP3 inflammasome assembly and activation. However, this inhibition is independent of AA147-induced ATF6 activation. Instead, AA147 blocks inflammasome assembly and activation through a mechanism involving covalent modification of PDIA1 – a highly abundant ER PDI. Genetic depletion of *PDIA1* mimics AA147-depenent inflammasome inhibition. We also demonstrate that highly selective PDIA1 inhibitors show potent activity against NLRP3 inflammasome activation. These results identify PDIA1 as a novel target for inhibiting inflammasome signaling that could be potentially exploited for the continued development of next generation inflammasome inhibitors.

Results

AA147 Reduces NLRP3 Assembly and Activity

We initially sought to define the potential for the metabolically activated pro-drug AA147 to inhibit NLRP3 inflammasome assembly. We employed a recently described, high content imaging-based screening assay of inflammasome assembly that utilizes the human monocyte cell line THP1 expressing the inflammasome subunit ASC fluorescently tagged with GFP (ASC-GFP) under control of an NFκB-regulated promoter.[31] Inflammasome assembly can be monitored in these cells by following the formation of ASC-GFP puncta, or ‘specks’, that accumulate in response to treatment with both a priming stimulus (e.g., LPS) and an activating stimulus (e.g., nigericin, ATP). Treatment with both LPS and nigericin robustly increases ASC-GFP speck formation in undifferentiated THP1 cells (Figure 1A,B). Pre-treatment with the known NLRP3 inflammasome inhibitor MCC950[23] inhibited ASC-GFP speck formation. Interestingly, pre-treatment with AA147 similarly blocked ASC-GFP speck formation in undifferentiated THP1 cells, indicating that this compound inhibits inflammasome assembly.

Inflammasome activation leads to the increased secretion of the pro-inflammatory cytokine IL-1β.[7] Thus, we sought to determine the extent to which AA147 blocks this activity downstream of inflammasome assembly. Initially, we monitored secretion of IL-1β from monocyte THP1 cells using HEK-Blue IL-1β reporter cells (Invivogen) – a cell line that

expresses the IL-1β receptor and an NFκB-responsive secreted alkaline phosphatase (SEAP) reporter. Treatment of HEK-Blue IL-1β cells with conditioned media prepared on THP1 cells stimulated with LPS and nigericin increased secretion of SEAP, reflecting increased IL-1β secretion (Figure 1C). Treatment of THP1 cells with MCC950 blocked this effect, confirming that the increase in SEAP corresponds to NLRP3 inflammasome-dependent increases in IL-1β secretion from THP1 cells. AA147 similarly blocked IL-1β secretion from undifferentiated THP1 cells stimulated with LPS and nigericin (Figure 1C). Similar results were observed in THP1 monocyte-derived macrophages stimulated with LPS and ATP, as measured by both the HEK-Blue IL-1β reporter assay (Figure S1B) and an enzyme-linked immunoassay (ELISA) of conditioned media (Figure 1D). Further, AA147 reduced IL-1β in conditioned media prepared on RAW264.7 mouse macrophages stimulated with LPS and ATP, as measured by immunoblotting (Figure S1C). These results indicate that AA147 reduces NLRP3 inflammasome assembly and activity.

AA147-Dependent Inhibition of Inflammasome Activation is Independent of ATF6 Activation or NFκB Inhibition

AA147 was originally identified as an activator of the ATF6 signaling arm of the unfolded protein response.[32] Thus, we sought to determine the potential for AA147 to inhibit inflammasome activity through an ATF6-dependent mechanism. Surprisingly, we did not observe significant increases of the ATF6-target BiP in immunoblots prepared from THP1 cells treated for 16 h with AA147, indicating that this compound did not significantly increase ATF6 signaling in these cells (Figure S2A). Further, co-treatment with the ATF6 inhibitors Ceapin-A7[37] or the site 1 protease inhibitor PF429242[38] did not decrease AA147-dependent reductions of IL-1β secretion in monocyte THP1 cells stimulated with LPS and ATP (Figure 2A,B). These results indicate that AA147 does not reduce NLRP3 inflammasome-dependent IL-1β secretion through an ATF6-dependent mechanism.

AA147 could also influence inflammasome activation through suppression of NFκB-dependent expression of inflammasome components and pro-IL-1β. AA147 modestly reduced expression of *IL1B* in THP1 monocyte derived macrophages stimulated with LPS (Figure 2C), although this reduction was not detectable in naïve THP1 cells which showed a less dynamic response to LPS (Figure S2B). Further, AA147 did not impact the expression of other NLRP3 inflammasome subunits in differentiated THP1 cells (e.g., *ASC*, *NLRP3*, *CASP1*) (Figure S2C). A positive control MG132, which inhibits NFκB transcriptional activity by preventing its nuclear translocation, reduced the expression of the NFκB target genes *IL1B*, *ASC*, and *NLRP3* in both differentiated and undifferentiated THP1 cells (Figure 2C, S2B). We also did not observe changes in the protein levels for NLRP3 subunits or pro-IL-1β in differentiated THP1 cells stimulated with LPS and treated with AA147 (Figure 2D). This suggests that AA147 does not significantly impact expression of inflammasome subunits or pro-IL-1β in these cells.

Genetic Depletion of PDIA1 Inhibits Inflammasome Assembly and Activation

AA147 activates ATF6 through a mechanism involving metabolic activation and direct covalent modification of a subset of ER protein disulfide isomerases (PDIs).[33] Previous results showed that AA147-dependent inhibition of PDIs could promote adaptive ER

remodeling independent of ATF6 to influence secretion of destabilized, amyloidogenic immunoglobulin light chains.[34] Thus, we sought to determine if NLRP3 inflammasome activation and assembly could also be explained by AA147-dependent PDI inhibition. We used an alkyne-containing analog of AA147 ($AA147^{alk}$)[33] to confirm that AA147 covalently modified PDIs in monocyte THP1 cells (Figure S3A). We then shRNA-depleted the predominant PDIs modified by AA147, including *PDIA1*, *PDIA3*, *PDIA4*, *PDIA5*, and *PDIA6*,[33,34] in THP1 cells stimulated with LPS and ATP or nigericin and then monitored IL-1β secretion using the HEK-Blue IL-1β reporter assay. We confirmed efficient knockdown of individual PDIs by qPCR (Figure S3B). While depletion of all tested PDIs show modest inhibition of IL-1β secretion from THP1 cells stimulated with LPS and either nigericin or ATP, the most significant effects were observed upon knockdown of *PDIA1* and *PDIA5* (Figure 3A). We specifically focused on PDIA1, as this PDI is highly modified by AA147 across multiple cell types, whereas PDIA5 has not been identified as a robust target across cell types.[33,34,36] Additionally, CRISPR-mediated ablation of PDIA1 diminishes secretion of pro-inflammatory cytokines in other cell types, implicating PDIA1 as a potential regulator of inflammatory signaling.[39]

We confirmed that PDIA1 mRNA and protein expression was reduced in THP1 cells stably depleted of *PDIA1* (Figure S3C, D, respectively). Importantly, we also showed that *PDIA1*-depletion did not increase expression of the UPR target gene BiP, indicating that reduced activity of PDIA1 does not globally induce ER stress in these cells. As with AA147 pretreatment, *PDIA1* depletion reduced ASC-GFP speck formation in THP1 cells stimulated with LPS and nigericin (Figure 3B). Further, we found that *PDIA1* depletion inhibited autoproteolysis of caspase 1 (Figure 3C,D) – another marker of inflammasome assembly and activation.[7,40] *PDIA1* depletion showed a modest reduction in *IL1B* expression in LPS stimulated THP1 monocytes, although no effect was observed for the NLRP3 inflammasome subunits *NLRP3* or *ASC* (Figure S3C). However, we did not observe significant reductions in pro-IL-1β in THP1 cells depleted of *PDIA1* (Figure 3E). Instead, pro- IL-1β levels trended toward increasing, although this was not found to be a statistically significant change in expression. Overall, these results indicate that *PDIA1* depletion inhibits NLRP3 inflammasome assembly and activation through a mechanism analogous to that observed with AA147.

Selective, Pharmacologic PDIA1 Inhibitors Block Inflammasome Assembly and Activation

The above results suggest that AA147 inhibits NLRP3 assembly and activation through covalent targeting of PDIs, most notably PDIA1. This suggests that other PDIA1 inhibitors should similarly inhibit NLRP3 inflammasome assembly and activation. To test this, we monitored ASC-GFP speck formation in monocyte THP1 cells treated with the highly selective, covalent PDIA1 inhibitor KSC-34[41] and stimulated with LPS and nigericin. KSC-34 contains an alkyne moiety, allowing us to confirm efficient engagement of PDIA1 by this compound (Figure 4A, B). Treatment with KSC-34 significantly reduced ASC-GFP speck formation induced by LPS and nigericin (Figure 4C). Further, KSC-34 reduced IL-1β secretion in THP1 cells stimulated with LPS and nigericin, as measured by HEK-Blue IL-1β reporter assay (Figure S4A). Similar results were observed in THP1 cells stimulated with LPS and ATP (Figure 4D). The structurally analogous PDIA1 inhibitor RB-11-CA[41]

also demonstrated reduced IL-1β secretion from monocyte THP1 cells (Figure 4A,B,D). Further, we confirmed that these two PDIA1 inhibitors did not directly label NLRP3, unlike the recently identified NLRP3 covalent modifier P207–9174 (Figure S4B).[31] Lastly, we demonstrated that neither AA147 nor KSC-34 showed additional reduction in IL-1β secretion, measured by HEK- IL-1β reporter assay, from THP1 cells depleted of *PDIA1* and stimulated with LPS and nigericin (Figure S4C). This indicates that these inhibit inflammasome activity through a *PDIA1*-dependent mechanism.

Discussion

Pharmacologic interventions which suppress the NLRP3 inflammasome activity show significant promise in mitigating the harmful effects of persistent or excessive inflammation.[7,16,17] Here, we show that the metabolically activated electrophile AA147 can suppress pro-inflammatory IL-1β signaling by inhibiting assembly of the NLRP3 inflammasome. Although AA147 was initially characterized as a preferential activator of the ATF6 arm of the UPR,[32] the inhibition of IL-1β secretion was not dependent on ATF6 signaling. Instead, we show that AA147 impedes inflammasome activity through the covalent modification of PDIs, specifically PDIA1. Genetic ablation of *PDIs*, most notably *PDIA1*, showed similar results to AA147. Importantly, knockdown of *PDIA1* inhibited inflammasome assembly, caspase 1 proteolytic autoactivation, and IL-1β secretion – highlighting the extent to which PDIA1 is involved in NLRP3 inflammasome signaling. Furthermore, selective and structurally distinct inhibitors of PDIA1 similarly reduced assembly of the inflammasome complex as well as IL-1β secretion. Overall, these results indicate that indirectly suppressing inflammasome activation by targeting proteins which regulate NLRP3 inflammasome oligomerization, such as PDIA1, may represent a novel strategy for reducing the pathologic impacts of inflammasome overactivation.

While it remains unclear how PDIA1 interacts with inflammasome assembly, the central role of PDIA1 in ER stress,[42,43] ROS generation,[44,45] and disulfide bond formation[41,45] – all factors which can impact NLRP3 inflammasome localization and assembly[35,46–48] – suggest that PDIA1 could impact NLRP3 complex assembly and IL-1β secretion at multiple stages of inflammasome activation. Consistent with this, a number of studies have demonstrated that PDIA1 can regulate pathologic inflammatory signaling through diverse mechanisms involving both direct and indirect modes of action. While PDIA1 is generally considered a resident chaperone localized to the ER,[41,43] a few studies have shown cytosolic PDIA1 interactions[49] and it has been widely reported to localize at the cell surface and extracellularly.[41,42,49] Previous studies have shown that extracellular PDI is an important regulator of innate immune activity as it can modulate the extent of neutrophil adhesion by impacting the surface expression of molecules including L-selectin[50] and integrins[51–54] through direct interactions. Blocking antibodies have shown that PDIs localized to the cell surface may also be indirectly involved in the release of tissue factor and IL-1β from macrophages by regulating the thiol-dependent release of microparticles containing inflammatory cytokines.[55] CRISPR knockdown of PDIA1 has also been shown to limit the extent of LPS-induced reactive oxygen species (ROS) to suppress NFκB activity to reduce the secretion of the inflammatory cytokines IL-6 and TNFα.[39]

In our study, we used structurally distinct pharmacologic inhibitors of PDIA1 as well as shRNA-mediated silencing to show that PDIA1 can also regulate the processing and release of the potent pro-inflammatory cytokine IL-1β by preventing NLRP3 inflammasome assembly. These studies suggest that PDIA1 activity may be a central regulator of inflammatory signaling across myeloid cell lineages through a diverse range of intracellular and extracellular signaling mechanisms. Therefore, further exploration of the potential of PDI inhibition to mitigate damaging inflammation may present new opportunities to improve patient outcomes across a wide range of disorders.

Methods

Cell Culture Maintenance and shRNA Depletion

The THP1 cells (THP1 null; Invivogen) were a generous gift from the Griffin lab at Scripps Research and the ASC-GFP THP1 (Invivogen) cells were a generous gift from CALIBR. THP1 cell lines were maintained in RPMI 1640 (ATCC formulation, LifeTech cat. A1049101) supplemented with 10 % heat-inactivated fetal bovine serum (FBS) (Lifetech cat. 10082147), 100 μg/ml Normocin (Invivogen cat. ant-nr-1) and Pen-Strep (100 μg/ml). Alternating passages of THP1 cells were treated with 200 μg/ml Hygromycin Gold (Invivogen cat. ant-hg-1) as recommended by Invivogen. ASC-GFP THP1 cells were passaged with 100 μg/ml Zeocin (Fisher Scientific cat. AAJ67140XF). Selection media was fully removed prior to inflammasome stimulation.

THP1 cells were differentiated into macrophages by treating 1 M cells/mL with 0.5 μM phorbol 12-myristate 13-acetate (PMA; Sigma; cat P8139) for 3 h on Day 0. After the initial media change following PMA, media was refreshed daily for two additional days. On Day 2, compounds were added to media for pre-treatment. The following day, THP1 derived macrophages were stimulated with inflammasome priming and activation stimuli; compound was readded to media with each media change after initial pre-treatment.

For shRNA depletion, viruses expressing specific shRNAs were prepared as previously described.[38] Briefly, one 10 cm dish of HEK293T cells per shRNA was transiently transfected with 8 μg shRNA construct, 4 μg REV (pRSV-rev), 4 μg RRE (pMDL-RRE), and 4 μg VSV—G (pMD2.G). Transfection reagents were removed after a 24 h incubation, followed by a 24 h incubation for viral production in THP1 cell media. A 1:1 ratio of virus-containing media and fresh media was added to THP1 cells or ASC-GFP THP1 cells for 24 h. Transfected cells were puromycin-selected (5 μg/L) (Sigma-Aldrich; cat P8833) for 7 days. Knockdown was confirmed by real-time quantitative polymerase chain reaction (RT-qPCR) and immunoblotting.

IL-1β Reporter HEK 293 cells were a kind gift from CALIBR and were cultured in DMEM supplemented with 10 % heat inactivated FBS (Lifetech cat. 10082147), 2 mM glutamine and Pen-Strep (100 μg/ml). Cells were subcultured in 100 μg/ml of Zeocin as recommended by manufacturer. Trypsin was not used to detach cells, as it can interfere with the secreted alkaline phosphatase (SEAP) reporter. HEK293T cells were cultured in high glucose DMEM (4.5 g/L) (Corning cat. 15–017-CV) supplemented with 10 % FBS and Pen-Strep (100 μg/ml).

Compounds and Treatments

Ultra-pure TLR4 specific lipopolysaccharide derived from *E. coli* strain 0111:B4 (LPS; Invivogen cat. tlrl-3pelps) at a dose of 1 μg/mL was used to induce NFκB transcription activity for inflammasome priming across all experiments. Inflammasome assembly was induced by administering cells with 5 mM ATP (Jena Biosciences cat. NU-1010) or nigericin (Invivogen cat. tlrl-nig) with dose, as indicated.

AA147 and AA147^{alk} were previously reported[33] and kind gifts from the Kelly Lab at Scripps Research, suspended in dimethyl sulfoxide (DMSO), and administered at 10 μM. PF429242 (Sigma-Aldrich; cat. SML0667) was resuspended in water and administered at 10 μM. CP7 was obtained from the Walter Lab at UCSF, resuspended in DMSO, and administered at 6 μM. RB-11-CA and KSC-34 were previously reported[41] and were kind gifts from the Weerapana Lab at Boston College. Compounds were resuspended in DMSO and administered at 20 μM. MCC950 (Selleck Chem; cat. S7809) was resuspended in water and administered at 1 μM concurrently with the addition of LPS for all experiments. Z-VAD-FMK was administered at 50 μM at the same time as the secondary stimulus.

Plasmids and Antibodies

For viral transfection, the following plasmids were used: REV (pRSV-rev; Addgene cat. 12253), RRE (pMDL-RRE; Addgene cat. 12251), and VSV—G (pMD2. G; Addgene cat. 12259). Mission shRNA plasmids in pLKO.1 vectors were obtained from La Jolla Institute for Allergy and Immunology (LJI) and were previously used in Paxman et al.38 The specific target sequences for viral plasmid of these shRNAs are below:

The following primary antibodies were diluted as noted in 5 % bovine serum albumin (BSA) in TBS and incubated overnight: KDEL (1 : 1000; Enzo cat. ADI-SPA-827-F), NLRP3 (1 : 1000; Cell Signaling cat. 15101), CASP1 (1 : 1000; Cell Signaling cat. 3866), ASC (1 : 1000, Cell Signaling cat. 13833), IL-1β (1 : 1000, GeneTex cat. GTX74034), PDIA1 (1 : 1000, Cell Signaling cat. 45596), Tubulin (1 : 2000; Sigma-Aldrich T6074), GAPDH (1 : 1000, GeneTex cat. GTX627408), NEK7 (1 : 1000, Cell Signaling cat. 3057).

Inflammasome Assembly Assay

ASC. GFP THP1 cells were plated at a density of 20,000 cells / well in a 384 well plate and treated with compounds for 16 h. Cells were then primed with LPS (1 μg/mL) for either 3 h or 16 h as noted. Subsequently, cells were stimulated with nigericin (10 μM) for 3 hours. Nuclei were stained using 5 μg/mL Hoechst 33342 (Thermo cat. H3570). Images were captured using Cellomics Cell Insight imaging reader (Thermo). An air ×10 lens was used to capture one image per well. For image analysis, stained nuclei were enumerated as representing the total number of live cells captured. ASC-GFP speck formation was calculated using an algorithm within the Cell Insight software, which factors both signal intensity and area size. Numerical results from the analyzed images were later exported for analysis using Prism 9 (GraphPad, San Diego, CA)

Target (Designation)	shRNA sequence
PDIA1	CCGGGTGTGGTCACTGCAAACAGTTCTCGAGAACTGTTTGCAGTGACCACACTTTTTG
PDIA3	CCGGCCAACACTAACACCTGTAATACTCGAGTATTACAGGTGTTAGTGTTGGTTTTTTG
PDIA4-1	CCGGCTTGGTCCTAAATGATGCAAACTCGAGTTTGCATCATTTAGGACCAAGTTTTTG
PDIA4-2	CCGGGCTTGTGTTGACCAAAGAGAACTCGAGTTCTCTTTGGTCAACACAAGCTTTTTG
PDIA5-1	CCGGGCTCCTGAAGAAGGAAGAGAACTCGAGTTCTCTTCCTTCTTCAGGAGCTTTTTG
PDIA5-2	CCGGCCTGGCAGAAAGATTCCACATCTCGAGATGTGGAATCTTTCTGCCAGGTTTTTG
PDIA6-1	CCGGGAGATTATCAACGAGGACATTCTCGAGAATGTCCTCGTTGATAATCTCTTTTTG
PDIA6-2	CCGGGCAGATAAGCATCATTCCCTACTCGAGTAGGGAATGATGCTTATCTGCTTTTTG

IL-1β Assays

Undifferentiated THP1 cells were plated in fresh media at a density of 750 K/mL and compounds were concurrently administered, as noted. The following day, cells were stimulated using LPS (1 μg/mL) for 3 h and then ATP (5 mM) or nigericin (1 μM) were added directly to the cells. Cells were incubated at 37o for 24 h following the addition of the secondary stimulus. Cells and conditioned media were centrifuged at a low speed to remove suspended monocytes. The supernatant was added IL-1β Reporter HEK 293 Cells (Invivogen cat. hkb-il1bv2) following the manufacturer's protocol. Quanti-blue (Invivogen cat. rep-qbs) was used to detect the levels of the secreted alkaline phosphatase reporter following manufacturer's protocol. Absorbance was measured using SPECTRAmax PLUS 384 (Molecular Devices) plate reader at OD630.

For assays performed on THP1 derived macrophages, macrophages were treated on day 3 for 3 h with Ultrapure TLR4 specific lipopolysaccharide derived from E. coli strain 0111:B4 (LPS; Invivogen cat. tlrl-3pelps). This media was changed and ATP (5 mM) (Jena Biosciences cat. NU-1010) was added for 24 h prior to collection of conditioned media. Conditioned media was added directly to the IL-1β Reporter HEK 293 cells. Media for the ELISA was immediately stored after collection at −80°C for subsequent testing in the enzyme-linked immunoassay (R&D systems). The Human IL-1β Quantikine ELISA Kit (R&D Systems cat. DLB50) was used to quantify levels of IL-1β according to the manufacturer's protocol. RAW264.7 cells were plated in the morning and pre-treated in the afternoon on the same day as plating. Cells were stimulated for 3 h with Ultrapure TLR4 specific lipopolysaccharide derived from E. coli strain 0111:B4 (LPS; Invivogen cat. tlrl-3pelps). This media was changed and ATP (5 mM) (Jena Biosciences cat. NU-1010) was added for 24 h prior to collection of conditioned media. IL-1β levels were detected in conditioned media using SDS-PAGE followed by immunoblotting.

ASC-GFP Flow Cytometry

ASC-GFP THP1 cells were plated at a density of 750 K cells/mL were plated in 100 μL in a 96 well plate. Cells were pre-treated for 16 h with AA147. The following day, cells were stimulated with LPS (1 μg/mL) for 3 h and immediately analyzed via flow cytometry on a NovoCyte 3000 (Acea). GFP fluorescence was detected using ex. 488 nm, em. 530/30 nm

channel. Analysis and gating were performed using FlowJo software (BD Biosciences, San Diego). A minimum of 10,000 cells per sample were used to calculate the geometric mean GFP signal.

Gene	Forward	Reverse
PDIA1	5'-CCAAGGAGAACCTGCTGGAC-3'	5'-CGGCTGCTGTTTTGAAGTTG-3'
PDIA2	5'-GGCCAGTTAAGACCCTCGTG-3'	5'-TGATGTCCTCGTGGTCTTGG-3'
PDIA3	5'-ATGCCCTAAGGATGGGTTCC-3'	5'-CCCAGCAGTGTCAGCAATTC-3'
PDIA4	5'-GGCCCACGAGAAAAATATGG-3'	5'-GCTGGTAGGCTGGGTCACTC-3'
PDIA5	5'-CCCGAAGGACAAAAAGGTG-3'	5'-CCAGGATCTTCCTCCCACAG-3'
PDIA6	5'-GGAGCACCAGCTCTGTGTTG-3'	5'-AGACTGGGCTCCAGCTTCTG-3'
IL1B	5'-AGCTCGCCAGTGAAATGATG-2'	5'-GGTGGTCGGAGATTCGTAGC-3'
CASP1	5'-GAGCTGAGGTTGACATCACAGG-3'	5'-TGCTGTCAGAGGTCTTGTGCT-3'
ASC	5'-GCTGCTGGATGCTCTGTACG-3'	5'-GTCCTTGCAGGTCCAGTTCC-3'
CCL5	5'- TCATTGCTACTGCCCTCTGC-3'	5'- CAAAGACGACTGCTGGGTTG-3'
NLRP3	5'- CTTCGATGAGCTGCAAGGTG-3'	5'- CAGGTCTCGTGGTGATGAGC-3'
RiboP	5'-CGTCGCCTCCTACCTGCT-3'	5'-CCATTCAGCTCACTGATAACCTTG-3'

Quantitative Reverse-Transcriptase Polymerase Chain Reaction (qRT-PCR)

Cells were rinsed with PBS, lysed, and total RNA was collected using the QuickRNA mini kit (Zymo) according to the manufacturer's instructions. The relative quantification of mRNA per sample was calculated using qPCR with reverse transcription (RT-qPCR) of the endogenous control RPLP2 (RiboP). RNA yield was quantified using Nanodrop. cDNA was generated from 300 ng of RNA using High-Capacity cDNA Reverse Transcription Kit (Advanced Biosystems; cat. 4368814). qPCR reactions were prepared using Power SYBR Green PCR Master Mix (Applied Biosystems; cat. 4367659), and primers were obtained from Integrated DNA Technologies. Amplification reactions were run in an ABI 7900HT Fast Real Time PCR machine with an initial melting period of 95°C for 5 min and then 45 cycles of 10 s at 95°C, 30 s at 60°C.

Bioluminescent Caspase 1 Cleavage Assay

The caspase 1 glo (Promega; cat. G9951) was followed according to manufacturer's instructions. Briefly, undifferentiated THP1 cells were plated at a density of 750 K cells/mL and treated for 16 h with LPS (1μg/mL) in a flask. The following day, cells were removed from LPS media, resuspended in fresh media at a density of 1 M cells/mL, and 25 μL of the suspension was plated in a 384 well dish. 20 μM Nigericin was added to individual wells for 45 minutes. Subsequently, caspase 1 reagent as well as the proteasome inhibitor MG132, and ac-YVAD were added to respective treatments and or controls. Reactions were incubated in the dark at room temperature for a minimum of 1 prior to luminescence being read on a Tecan F200 Pro microplate reader.

Rhodamine Labeling

Rhodamine-azide labeling reactions were performed in a 50 μL reaction containing 1.5 μg of protein from lysate from THP1 cell lysate treated with respective compounds for 16 h. Click reactions contained a final concentration of 0.8 mM CuSO4, 1.6 mM BTTAA (Sigma cat. 906328), 5 mM Sodium Ascorbate (Sigma cat. A4034), and 0.1 mM TAMRA azide (Santa Cruz cat. sc-482005). Reactions were incubated at 4oC overnight, then denatured with 1×Laemmli buffer+100 mM dithiothreitol (DTT) and boiled before being separated by SDS-PAGE. Gel was then stained with 0.1 % Coomassie Blue R250 in 10 % acetic acid/50 % methanol solution. Both rhodamine fluorescence and Coomassie staining were imaged on a ChemiDoc Imaging Systems (BioRad).

NLRP3 Labeling and Immunopurification

THP1 cells were treated with either KSC-34 or RB-11-CA for 16 h. Cell lysates were prepared via sonication in PBS. Biotin labeling reactions were performed using 1.7 mM TBTA, 50 mM CuSO4, 5 mM Biotin-PEG3-azide, and 50 mM tris(2-carboxyethyl)phosphine (TCEP). The protein was purified using MeOH precipitation, resuspended in 0.1 % SDS in PBS and streptavidin agarose slurry added. Streptavidin enrichment and elution was performed as previously described.[31]

SDS-Page and Immunoblotting

Briefly, cells were lysed in lysis buffer (50 mM Tris, pH 7.5, 150 mM NaCl, 20 mM Hepes pH 7.4, 1 mM EDTA, 1 % Triton X-100, and protease inhibitor cocktail (Pierce cat. A32955)). The total protein concentration in cellular lysates was normalized using the Bio-Rad protein assay. Lysates were then denatured with 1 × Laemmli buffer + 100 mM dithiothreitol (DTT) and boiled before being separated by SDS-PAGE. Samples were transferred onto nitrocellulose membranes (Bio-Rad cat. 1620112). Membranes were then incubated overnight at 4 °C with primary antibodies with dilutions, as noted. Membranes were washed in TBS—T, incubated with the species-appropriate IR-Dye conjugated secondary antibodies diluted at 1:10,000, and analyzed using the Odyssey Infrared Imaging System (LI–COR Biosciences). Quantification was carried out with LI–COR Image Studio software.

Supplementary Material

Refer to Web version on PubMed Central for supplementary material.

Acknowledgements

We thank John Griffin and Laura Healy at Scripps Research for experimental advice related to the work described in this manuscript. This work was funded by the National Institutes of Health (DK107604, AG046495 to RLW).

Data Availability Statement

The data that support the findings of this study are available from the corresponding author upon reasonable request.

References

[1]. Lamkanfi M, Dixit VM, Cell 2014, 157, 1013–1022. [PubMed: 24855941]

[2]. Gross O, Thomas CJ, Guarda G, Tschopp J, Immunol. Rev 2011, 243, 136–151. [PubMed: 21884173]

[3]. Kelley N, Jeltema D, Duan Y, He Y, Int. J. Mol. Sci 2019, 20, 3328. [PubMed: 31284572]

[4]. Broz P, Dixit VM, Nat. Rev. Immunol 2016, 16, 407–420. [PubMed: 27291964]

[5]. Netea MG, Nold-Petry CA, Nold MF, Joosten LAB, Opitz B, van der Meer JHM, van de Veerdonk FL, Ferwerda G, Heinhuis B, Devesa I, Funk CJ, Mason RJ, Kullberg BJ, Rubartelli A, van der Meer JWM, Dinarello CA, Blood 2009, 113, 2324–2335. [PubMed: 19104081]

[6]. Sharif H, Wang L, Wang WL, Magupalli VG, Andreeva L, Qiao Q, Hauenstein AV, Wu Z, Núñez G, Mao Y, Wu H, Nature 2019, 570, 338–343. [PubMed: 31189953]

[7]. Swanson KV, Deng M, Ting JPY, Nat. Rev. Immunol 2019, 19, 477–489. [PubMed: 31036962]

[8]. Tong Y, Wang Z, Cai L, Lin L, Liu J, Cheng J, Ox. Med. Cell Longev 2020, 2020, 4293206.

[9]. Dinarello CA, Blood 2011, 117, 3720–3732. [PubMed: 21304099]

[10]. Aday AW, Ridker PM, Front. Cardiovasc. Med 2018, 5, 62. [PubMed: 29922680]

[11]. Aksentijevich I, Putnam CD, Remmers EF, Mueller JL, Le J, Kolodner RD, Moak Z, Chuang M, Austin F, Goldbach-Mansky R, Hoffman HM, Kastner DL, Arthritis Rheum. 2007, 56, 1273–1285. [PubMed: 17393462]

[12]. Brydges SD, Mueller JL, McGeough MD, Pena CA, Misaghi A, Gandhi C, Putnam CD, Boyle DL, Firestein GS, Horner AA, Soroosh P, Watford WT, O'Shea JJ, Kastner DL, Hoffman HM, Immunity 2009, 30, 875–887. [PubMed: 19501000]

[13]. Mikkelsen RR, Hundahl MP, Torp CK, Rodríguez-Carrio J, Kjolby M, Bruun JM, Kragstrup TW, Eur. J. Pharmacol 2022, 925, 174998. [PubMed: 35533739]

[14]. Larsen CM, Faulenbach M, Vaag A, Vølund A, Ehses JA, Seifert B, Mandrup-Poulsen T, Donath MY, N. Engl. J. Med 2007, 356, 1517–1526. [PubMed: 17429083]

[15]. Ismael S, Zhao L, Nasoohi S, Ishrat T, Sci. Rep 2018, 8, 5971. [PubMed: 29654318]

[16]. Abbate A, Toldo S, Marchetti C, Kron J, Tassell BWV, Dinarello CA, Circ. Res 2020, 126, 1260–1280. [PubMed: 32324502]

[17]. Mangan MSJ, Olhava EJ, Roush WR, Seidel HM, Glick GD, Latz E, Nat. Rev. Drug Discovery 2018, 17, 588–606. [PubMed: 30026524]

[18]. Yang Y, Wang H, Kouadir M, Song H, Shi F, Cell Death Dis. 2019, 10, 128. [PubMed: 30755589]

[19]. Li Y, Huang H, Liu B, Zhang Y, Pan X, Yu X-Y, Shen Z, Song Y-H, Signal Transduct Target Ther. 2021, 6, 247. [PubMed: 34210954]

[20]. Lythgoe MP, Prasad V, Br. J. Cancer 2022.

[21]. Ridker PM, Everett BM, Thuren T, MacFadyen JG, Chang WH, Ballantyne C, Fonseca F, Nicolau J, Koenig W, Anker SD, Kastelein JJP, Cornel JH, Pais P, Pella D, Genest J, Cifkova R, Lorenzatti A, Forster T, Kobalava Z, Vida-Simiti L, Flather M, Shimokawa H, Ogawa H, Dellborg M, Rossi PRF, Troquay RPT, Libby P, Glynn RJ, N. Engl. J. Med 2017, 377, 1119–1131. [PubMed: 28845751]

[22]. Coll RC, Hill JR, Day CJ, Zamoshnikova A, Boucher D, Massey NL, Chitty JL, Fraser JA, Jennings MP, Robertson AAB, Schroder K, Nat. Chem. Biol 2019, 15, 556–559. [PubMed: 31086327]

[23]. Coll RC, Robertson AA, Chae JJ, Higgins SC, Muñoz-Planillo R, Inserra MC, Vetter I, Dungan LS, Monks BG, Stutz A, Croker DE, Butler MS, Haneklaus M, Sutton CE, Núñez G, Latz E, Kastner DL, Mills KH, Masters SL, Schroder K, Cooper MA, O'Neill LA, Nat. Med 2015, 21, 248–255. [PubMed: 25686105]

[24]. van Hout GP, Bosch L, Ellenbroek GH, de Haan JJ, van Solinge WW, Cooper MA, Arslan F, de Jager SC, Robertson AA, Pasterkamp G, Hoefer IE, Eur. Heart J 2017, 38, 828–836. [PubMed: 27432019]

[25]. Primiano MJ, Lefker BA, Bowman MR, Bree AG, Hubeau C, Bonin PD, Mangan M, Dower K, Monks BG, Cushing L, Wang S, Guzova J, Jiao A, Lin L-L, Latz E, Hepworth D, Hall JP, J. Immunol 2016, 197, 2421–2433. [PubMed: 27521339]

[26]. Marchetti C, Swartzwelter B, Gamboni F, Neff CP, Richter K, Azam T, Carta S, Tengesdal I, Nemkov T, D'Alessandro A, Henry C, Jones GS, Goodrich SA, St. Laurent JP, Jones TM, Scribner CL, Barrow RB, Altman RD, Skouras DB, Gattorno M, Grau V, Janciauskiene S, Rubartelli A, Joosten LAB, Dinarello CA, Proc. Natl. Acad. Sci. USA 2018, 115, E1530–E1539. [PubMed: 29378952]

[27]. Klück V, Jansen T, Janssen M, Comarniceanu A, Efdé M, Tengesdal IW, Schraa K, Cleophas MCP, Scribner CL, Skouras DB, Marchetti C, Dinarello CA, Joosten LAB, Lancet Rheumatol 2020, 2, e270–e280. [PubMed: 33005902]

[28]. He H, Jiang H, Chen Y, Ye J, Wang A, Wang C, Liu Q, Liang G, Deng X, Jiang W, Zhou R, Nat. Commun 2018, 9, 2550. [PubMed: 29959312]

[29]. Chen Y, He H, Lin B, Chen Y, Deng X, Jiang W, Zhou R, Cell. Mol. Immunol 2021, 18, 1425–1436. [PubMed: 33972740]

[30]. Hooftman A, Angiari S, Hester S, Corcoran SE, Runtsch MC, Ling C, Ruzek MC, Slivka PF, McGettrick AF, Banahan K, Hughes MM, Irvine AD, Fischer R, O'Neill LAJ, Cell Metab. 2020, 32, 468–478.e467. [PubMed: 32791101]

[31]. Stanton C, Sun J, Nutsch K, Rosarda JD, Nguyen T, Li-Ma C, Kutseikin S, Saez E, Teijaro JR, Wiseman RL, Bollong MJ, bioRxiv 2023.

[32]. Plate L, Cooley CB, Chen JJ, Paxman RJ, Gallagher CM, Madoux F, Genereux JC, Dobbs W, Garza D, Spicer TP, Scampavia L, Brown SJ, Rosen H, Powers ET, Walter P, Hodder P, Wiseman RL, Kelly JW, eLife 2016, 5.

[33]. Paxman R, Plate L, Blackwood EA, Glembotski C, Powers ET, Wiseman RL, Kelly JW, eLife 2018, 7.

[34]. Rius B, Mesgarzadeh JS, Romine IC, Paxman RJ, Kelly JW, Wiseman RL, Blood Advances 2021, 5, 1037–1049. [PubMed: 33599742]

[35]. Zhou R, Yazdi AS, Menu P, Tschopp J, Nature 2011, 469, 221–225. [PubMed: 21124315]

[36]. Rosarda JD, Baron KR, Nutsch K, Kline GM, Stanton C, Kelly JW, Bollong MJ, Wiseman RL, ACS Chem. Biol 2021, 16, 2852–2863. [PubMed: 34797633]

[37]. Gallagher CM, Walter P, eLife 2016, 5.

[38]. Hawkins JL, Robbins MD, Warren LC, Xia D, Petras SF, Valentine JJ, Varghese AH, Wang IK, Subashi TA, Shelly LD, Hay BA, Landschulz KT, Geoghegan KF, Harwood HJ Jr., J. Pharmacol. Exp. Ther 2008, 326, 801–808. [PubMed: 18577702]

[39]. Xiao Y, Li C, Gu M, Wang H, Chen W, Luo G, Yang G, Zhang Z, Zhang Y, Xian G, Li Z, Sheng P, Inflammation 2018, 41, 614–625. [PubMed: 29294242]

[40]. O'Brien M, Moehring D, Muñoz-Planillo R, Núñez G, Callaway J, Ting J, Scurria M, Ugo T, Bernad L, Cali J, Lazar D, Immunol J. Methods 2017, 447, 1–13.

[41]. Cole KS, Grandjean JMD, Chen K, Witt CH, O'Day J, Shoulders MD, Wiseman RL, Weerapana E, Biochemistry 2018, 57, 2035–2043. [PubMed: 29521097]

[42]. Medinas DB, Rozas P, Hetz C, J. Biol. Chem 2022, 298.

[43]. Cao SS, Kaufman RJ, Antioxid. Redox Signaling 2014, 21, 396–413.

[44]. Ramming T, Okumura M, Kanemura S, Baday S, Birk J, Moes S, Spiess M, Jenö P, Bernèche S, Inaba K, Appenzeller-Herzog C, Free Radical Biol. Med 2015, 83, 361–372. [PubMed: 25697776]

[45]. Shergalis AG, Hu S, Bankhead A, Neamati N, Pharmacol. Ther 2020, 210, 107525. [PubMed: 32201313]

[46]. Menu P, Mayor A, Zhou R, Tardivel A, Ichijo H, Mori K, Tschopp J, Cell Death Dis. 2012, 3, e261–e261. [PubMed: 22278288]

[47]. Zhou Y, Tong Z, Jiang S, Zheng W, Zhao J, Zhou X, Cells 2020, 9, 1219. [PubMed: 32423023]

[48]. Rahman T, Nagar A, Duffy EB, Okuda K, Silverman N, Harton JA, Front. Immunol 2020, 11, 1828. [PubMed: 32983094]

[49]. Soares Moretti AI, Martins Laurindo FR, Arch. Biochem. Biophys 2017, 617, 106–119. [PubMed: 27889386]

[50]. Bennett TA, Edwards BS, Sklar LA, Rogelj S, J. Immunol 2000, 164, 4120–4129. [PubMed: 10754306]

[51]. Cho J, Kennedy DR, Lin L, Huang M, Merrill-Skoloff G, Furie BC, Furie B, Blood 2012, 120, 647–655. [PubMed: 22653978]

[52]. Hahm E, Li J, Kim K, Huh S, Rogelj S, Cho J, Blood 2013, 121, 3789–3800. [PubMed: 23460613]

[53]. Kim K, Hahm E, Li J, Holbrook L-M, Sasikumar P, Stanley RG, Ushio-Fukai M, Gibbins JM, Cho J, Blood 2013, 122, 1052–1061. [PubMed: 23788140]

[54]. Lahav J, Jurk K, Hess O, Barnes MJ, Farndale RW, Luboshitz J, Kehrel BE, Blood 2002, 100, 2472–2478. [PubMed: 12239158]

[55]. Furlan-Freguia C, Marchese P, Gruber A, Ruggeri ZM, Ruf W, J. Clin. Invest 2011, 121, 2932–2944. [PubMed: 21670495]

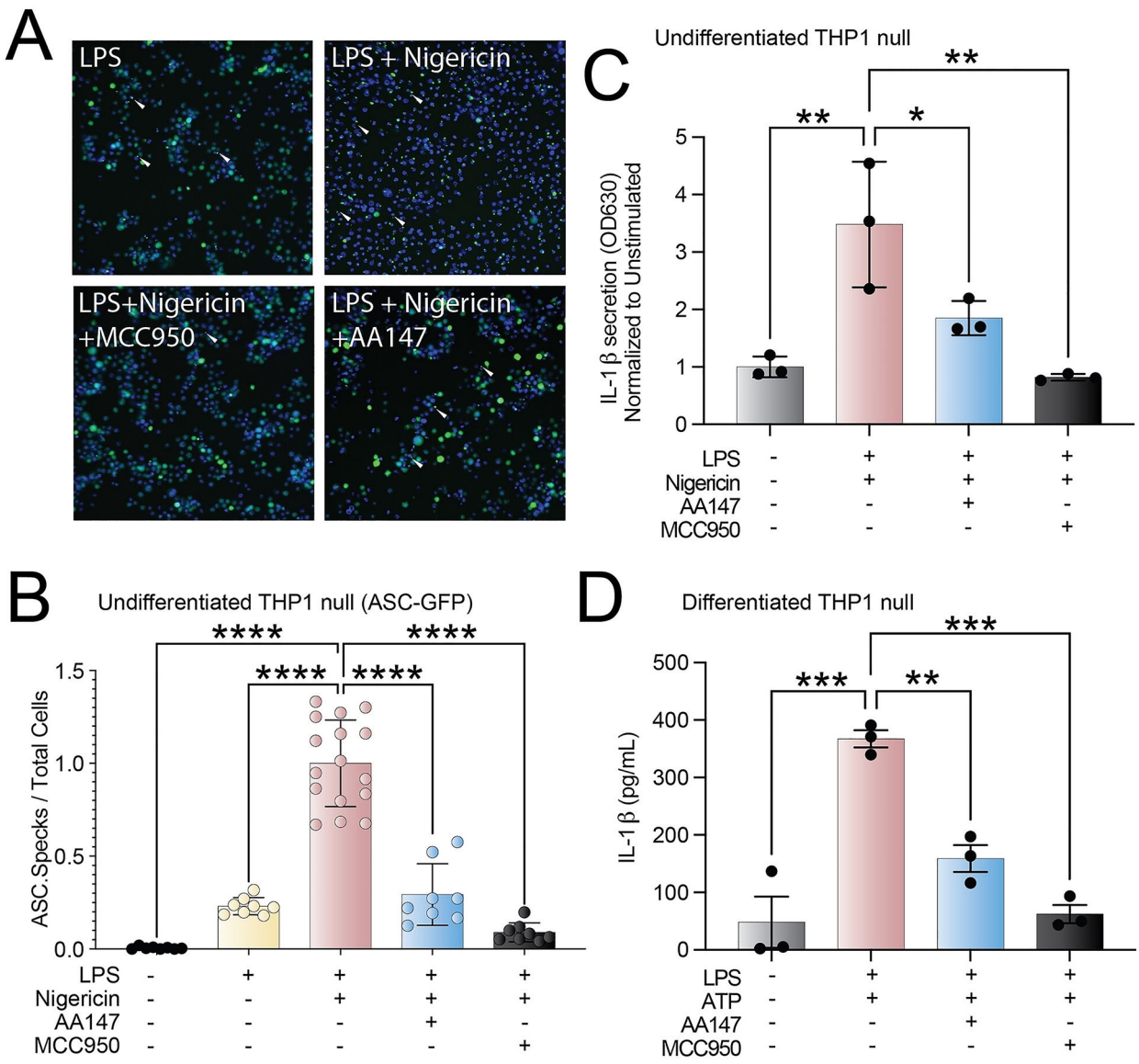

Figure 1. AA147 reduces NLRP3 inflammasome assembly and IL-1β secretion.

A. Representative fluorescent microscopy images of ASC-GFP cells untreated, treated with LPS (1 μg/mL) for 16 h ± nigericin (1 μM) 3 hours and in the presence or absence of AA147 (10 μM). ASC-GFP specks are indicated with white arrows. **B**. Quantification of images shown in (A). ****p<0.0001 using a Brown-Forsythe and Welch ANOVA test with Dunnett-T3 correction for multiple comparisons. Error bars show SD. **C**. Quantification of secreted bioactive IL-1β assessed using the SEAP Quanti-blue assay. HEK Blue IL-1β cells were treated with media conditioned on THP1 monocytes pre-treated with AA147 (10 μM) or vehicle for 16 h and stimulated with LPS (1 μg/mL) and nigericin (1 μM) for 24 h relative to an unstimulated, vehicle treated control. ****p<0.0001, ***p<0.001, **p<0.01 for one-way ANOVA test with Dunnett correction for multiple comparisons. Error bars show SEM for n=3. **D**. ELISA quantifications of total IL-1β detected in media conditioned on THP1 monocyte-derived macrophages pre-treated with AA147 (10 μM) or vehicle for 16

h then stimulated with LPS (1 μg/mL) for 3 h and incubated with ATP (5 mM) for 24 h. ***p<0.001, **p<0.01 for one-way ANOVA test with Dunnett correction for multiple comparisons. Error bars show SEM for n=3.

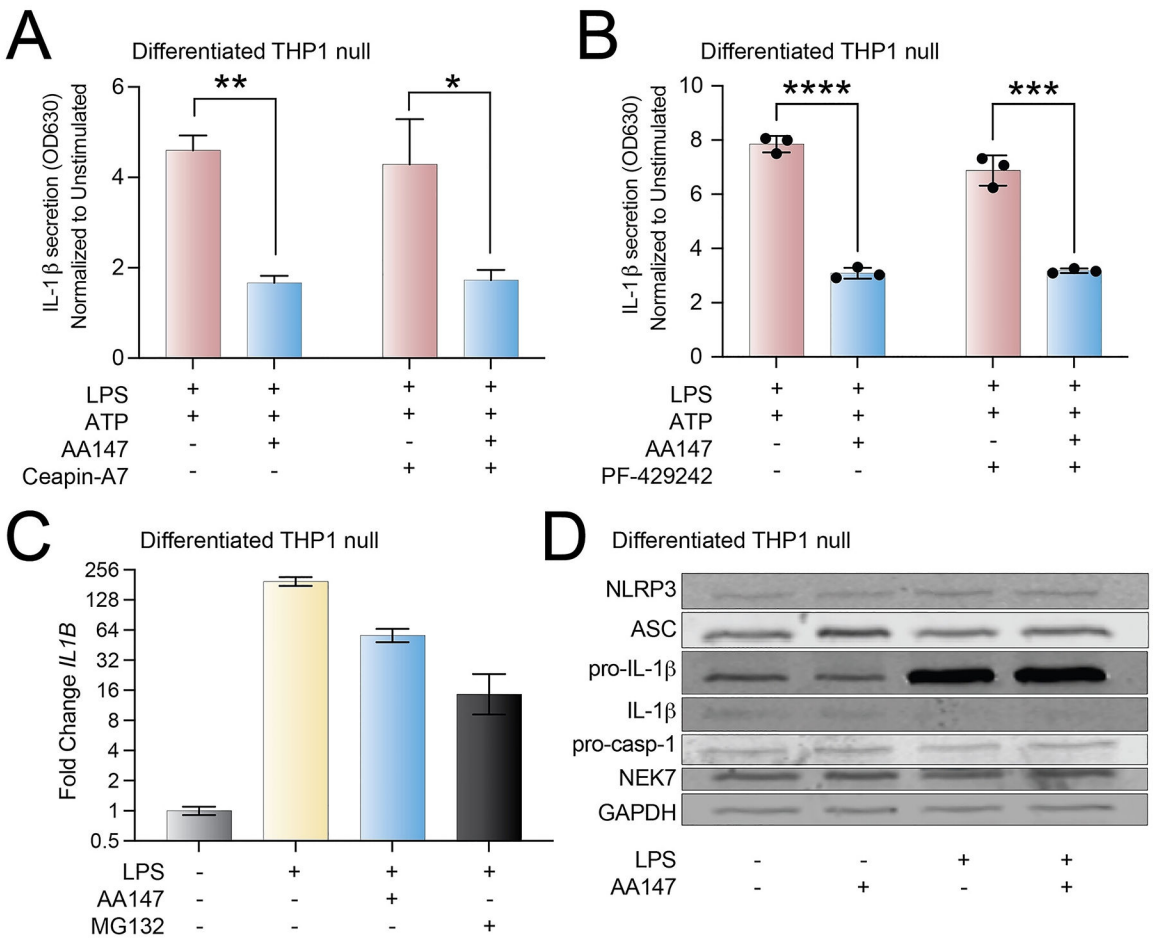

Figure 2. AA147-dependent inhibition of NLRP3 inflammasomes is independent of ATF6 activation.

A. Quantification of secreted bioactive IL-1β assessed using the SEAP Quanti-blue assay. HEK Blue IL-1β cells were treated with media conditioned on THP1 monocyte-derived macrophages pre-treated with AA147 (10 μM) or vehicle for 16 h in the presence or absence of the ATF6 inhibitor Ceapin-A7 (CP7; 6 μM) and subsequently stimulated for 3 h with LPS (1 μg/mL) and 24 h with ATP (5 mM). Results are relative to unstimulated, vehicle treated controls. ***p<0.001, ****p<0.0001 with multiple unpaired two-tailed t-tests. Error bars show SEM for n=3. **B**. Quantification of secreted bioactive IL-1β assessed using the SEAP Quanti-blue assay. HEK Blue IL-1β cells were treated with media conditioned on THP1 monocyte-derived macrophages pre-treated with AA147 (10 μM) or vehicle for 16 h in the presence or absence of the ATF6 inhibitor PF429242 (10 μM) and subsequently stimulated for 3 h with LPS (1 μg/mL) and 24 h with ATP (5 mM). Results are relative to unstimulated, vehicle treated controls. ***p<0.001, ****p<0.0001 with multiple unpaired two-tailed t-tests. Error bars show SEM for n=3. **C**. mRNA expression measured using qPCR, of the pro-inflammatory cytokine *IL1B* in THP1 monocyte-derived macrophages treated for 16 h with vehicle or AA147 (10 μM) and subsequently stimulated with LPS (1 μg/mL) for 3 h. Error bars show 95 % CI. **D**. Immunoblot of inflammasome components in

THP1 monocyte-derived macrophages pre-treated with vehicle or AA147 (10 μM) for 16 h and subsequently stimulated with vehicle or LPS (1 μg/mL) for 3 h.

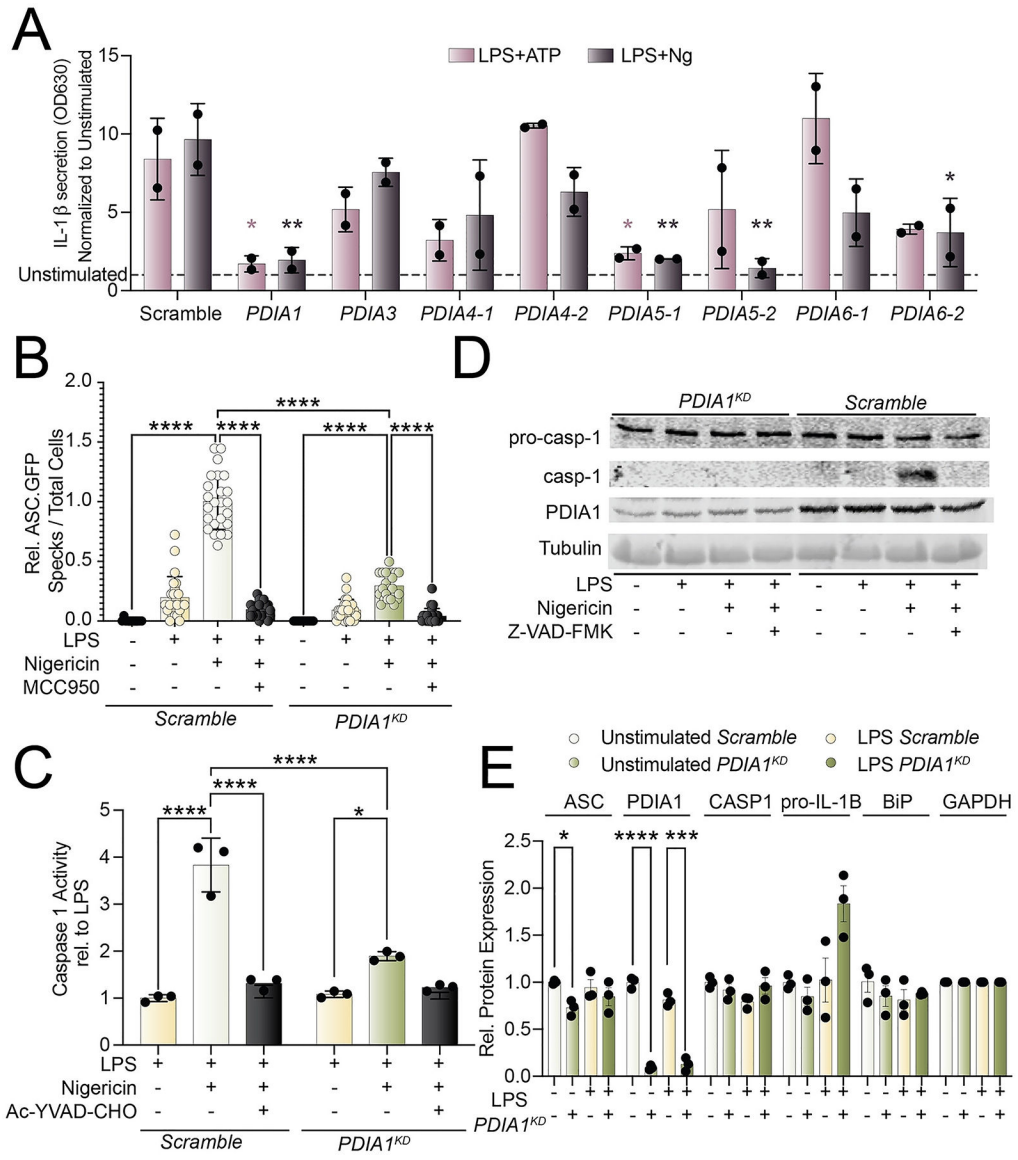

Figure 3. *PDIA1* depletion inhibits NLRP3 inflammasome activation.

A. Quantification of secreted bioactive IL-1β assessed using the SEAP Quanti-blue assay. HEK Blue IL-1β cells were treated with media conditioned on THP1 monocytes stably expressing shRNAs of the respective target PDI. were stimulated for 3 h with LPS (1 μg/mL) and 24 h with ATP (5 mM) or nigericin (1 μM). *p<0.05, ***p<0.001, ****p<0.0001 two-way ANOVA test with Dunnett correction for multiple comparisons. Error bars show SD. **B**. Relative number of ASC-GFP specks per cell detected using fluorescent microscopy in undifferentiated THP1 ASC-GFP monocyte cells stably expressing either a scramble shRNA or a PDIA1 shRNA (PDIA1^{KD}). Cells were stimulated with LPS (1 μg/mL) for 16 h and nigericin (5 μM) for 3 h. Quantification is relative to the overall average number of specks / total cells across all wells in LPS (1 μg/mL) and nigericin (5 μM) stimulated wells. ****p<0.0001 using a Brown-Forsythe and Welch ANOVA test with Dunnett-T3 correction for multiple comparisons. Error bars show SD. **C**. Caspase-1 activity assessed

using Caspase-1 Glo assay from PDIA1^{KD} or scramble THP1 monocytes stimulated for 16 h with LPS (1 μg/mL) and 45 min nigericin (1 μM). Error bars show SD; each dot represents an individual replicate relative to LPS. ****p<0.0001 using a two-way ANOVA. **D**. Immunoblot of cell lysates from PDIA1^{KD} or scramble THP1 cells stimulated with LPS (1 μg/mL) for 3 h and nigericin (5 μM) for 1 h. ZVAD-VAD-FMK (50 μM) was used as a positive control. **E**. Quantification of protein levels measured using immunoblots from cell lysates from *PDIA1^{KD}* or scramble THP1 cells stimulated with LPS (1 μg/mL) for 3 h. *p<0.05, ***p<0.001. ****p<0.0001 using multiple unpaired two-tailed t-tests. Error bars show SEM for n=3.

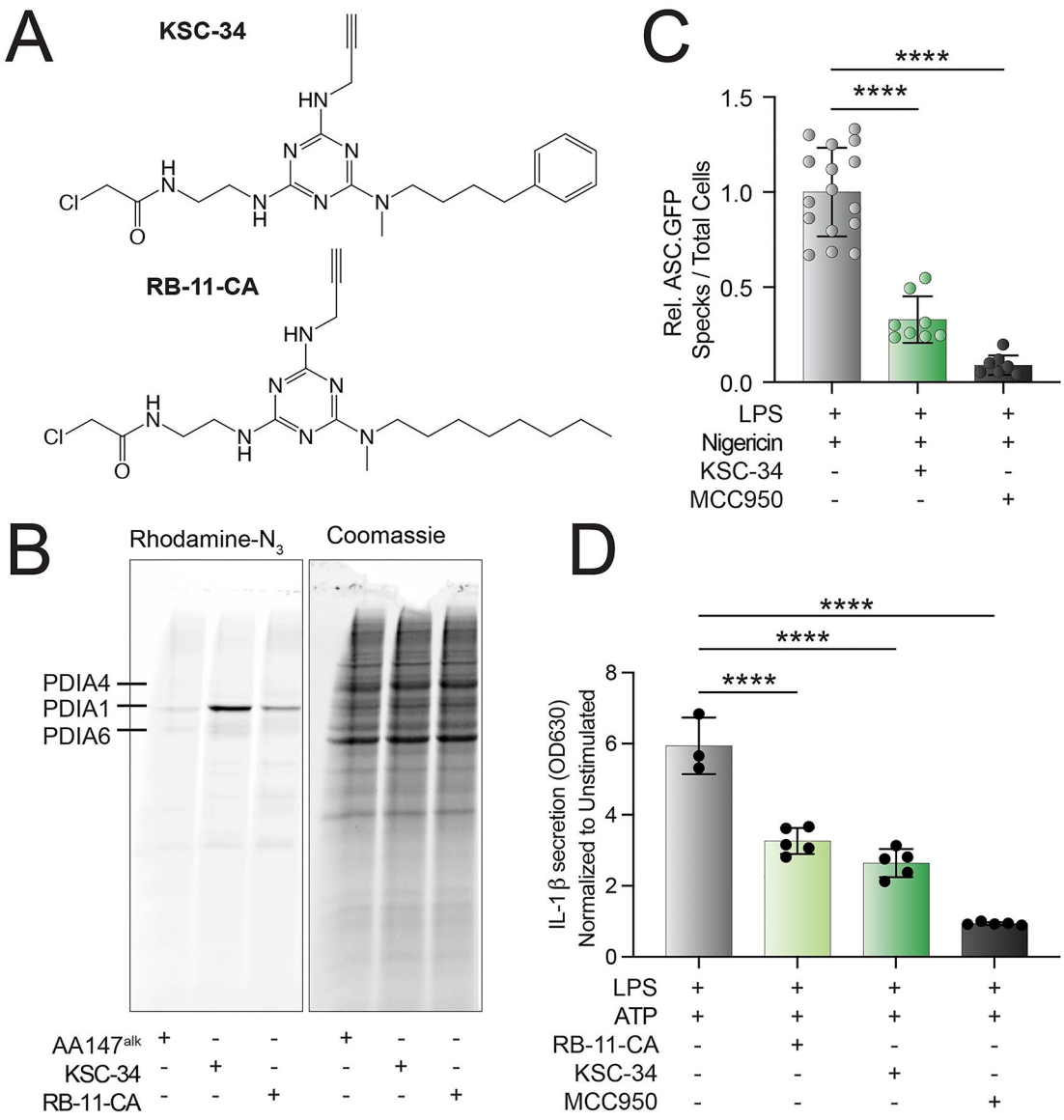

Figure 4. Pharmacologic PDI inhibitors block NLRP3 inflammasome activation.

A. Chemical structures of the PDI inhibitors KSC-34 and RB-11-CA.[41] **B**. Relative number of ASC-GFP specks per cell detected using fluorescent microscopy in undifferentiated THP1 ASC-GFP expressing monocyte cells pre-treated with KSC-34 (20 μM) and stimulated with LPS (1 μg/mL) for 16 h followed by a treatment of nigericin (5 μM) for 3 h. Quantification is relative to the overall average number of specks / total cells across all wells in LPS (1 μg/mL) and nigericin (5 μM) stimulated wells. ****p<0.0001 using a Brown-Forsythe and Welch ANOVA test with Dunnett-T3 correction for multiple comparisons. Error bars show SD. **B**. Rhodamine fluorescence and Coomassie staining of an SDS-PAGE gel of lysates from THP1 cells treated for 16 h with $AA147^{alk}$ (10 μM), KSC-34 (20 μM), or RB-11-CA (20 μM). **C**. Relative number of ASC-GFP specks per cell detected using fluorescent microscopy in undifferentiated THP1 ASC-GFP expressing monocyte cells pre-treated with KSC-34 (20 μM) for 16 h then stimulated with LPS (1 μg/mL) for 3 h and

nigericin for 3 h (5 μM). ****p<0.0001 using a Brown-Forsythe and Welch ANOVA test with Dunnett-T3 correction for multiple comparisons. Error bars show SD. **D**. Quantification of secreted bioactive IL-1β assessed using the SEAP Quanti-blue assay. HEK Blue IL-1β cells were treated with media conditioned on THP1 monocytes pre-treated with KSC-34 (20 μM) or RB-11-CA (20 μM) and subsequently stimulated for 3 h with LPS (1 μg/mL) and 24 h with nigericin (1 μM) relative to an unstimulated, vehicle treated control. *p< 0.05, ***p<0.001, ****p<0.0001 with one-way ANOVA test with Dunnett correction for multiple comparisons. Error bars show SEM for n=3.